Generation of a cone photoreceptor specific GNGT2 reporter line in human pluripotent stem cells

Liliya Nazlamova, Emma-Jane Cassidy, Jane C Sowden, Andrew Lotery, Jörn Lakowski

Generation of a cone photoreceptor specific GNGT2 reporter line in human pluripotent stem cells

Liliya Nazlamova[1], Emma-Jane Cassidy[2], Jane C Sowden[3], Andrew Lotery[1], Jörn Lakowski[1]

1. Clinical and Experimental Sciences, Clinical Neurosciences and Centre for Human Development, Stem Cells and Regeneration, Faculty of Medicine, University of Southampton, University Hospital Southampton, Southampton, UK

2. Wessex Regional Genetics Laboratory, Salisbury District Hospital, Salisbury, UK

3. Great Ormond Street Institute of Child Health, Stem Cells and Regenerative Medicine, Developmental Biology and Cancer Department. University College London, and NIHR Great Ormond Street Biomedical Research Centre, London, UK

Corresponding author

Dr Jörn Lakowski

Faculty of Medicine, Clinical Neurosciences, University of Southampton

LD70, Level D, South Academic Block, MP806, University Hospital Southampton

Southampton SO16 6YD; Tel: +44(0)23-8120-6418, email: j.lakowski@soton.ac.uk

Author contributions

Liliya Nazlamova: Acquisition of data and critically revised the manuscript

Emma-Jane Cassidy: Acquisition of data, analysis and interpretation

Jane C Sowden: data analysis and interpretation, manuscript writing, financial support

Andrew Lotery: data analysis and interpretation, manuscript writing

Jörn Lakowski: Conception and design, contributed to acquisition, analysis, and interpretation of data, drafted the manuscript, accountable for all aspects of work ensuring integrity and accuracy, financial support

Acknowledgements

This study was supported by The Academy of Medical Sciences Springboard Award (SBF004\1038), the Gift of Sight Appeal Elkington Fellowship in Vision Sciences, Fight for Sight UK; Great Ormond Street Hospital Charity. The views expressed are those of the author(s) and not necessarily those of the funders. We thank the Centre for Stem Cell Biology, The University of Sheffield, Sheffield, UK for ESC lines and Professor Hugh Perry for the useful discussions.

Conflict of interest

The authors declared no potential conflicts of interest.

Abstract

Fluorescent reporter lines generated in human pluripotent stem cells are a highly useful tool to track, isolate and analyse cell types and lineages in live cultures. Here, we generate the first human cone photoreceptor reporter cell line by CRISPR/Cas9 genome editing of a human embryonic stem cell (hESC) line to tag both alleles of the Guanine nucleotide-binding protein subunit gamma-T2 (GNGT2) gene with a mCherry reporter cassette. Three-dimensional optic vesicle-like structures were produced to verify reporter fidelity and track cones throughout their development in culture. The GNGT2-T2A-mCherry hESC line faithfully and robustly labels GNGT2-expressing cones throughout the entirety of their differentiation *in vitro*, recapitulating normal fetal expression of this gene. Our observations indicate that human cones undergo significant migratory activity during the course of differentiation *in vitro*. Consistent with this, our analysis of human fetal retinae from different stages of development finds positional differences of the cone population depending on their state of maturation. This novel reporter line will provide a useful tool for investigating human cone development and disease.

Keywords

Retinal organoids

Optic vesicles

GNGT2

Stem cells

Cone photoreceptor

Significance Statement

Human vision depends on photoreceptor cells located in the retina and conditions, which lead to their degeneration cause irreversible blindness. Rod photoreceptors are needed for night vision while cones mediate critical high acuity and colour vision. In this study, we engineered a human embryonic stem cell line, which expresses the fluorescent reporter mCherry under the control of the cone marker GNGT2 thereby enabling visualization, tracking and isolation of rare cone populations from 3D retinal organoids. This novel reporter line will provide a powerful tool for investigating human cone development and disease.

Graphical abstract

A human embryonic stem cell line was engineered to express the fluorescent marker mCherry in cone photoreceptors. Retinal organoids grown from these cells reveal extensive post-mitotic migratory activity of human cones consistent with observations in the human fetal retina.

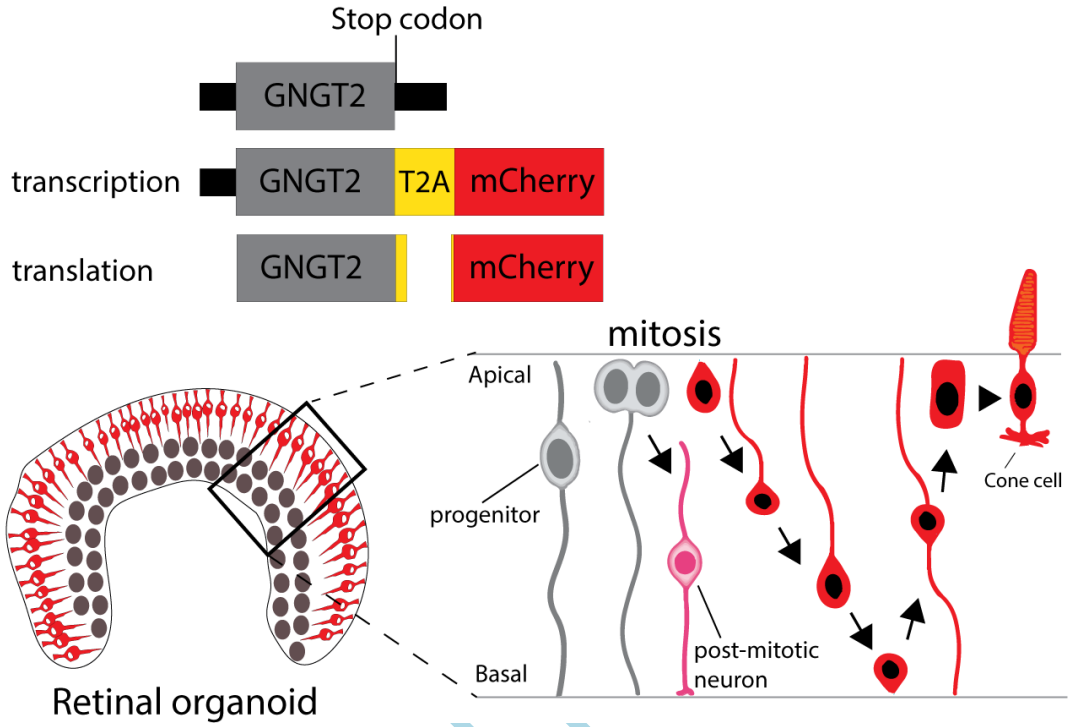

Introduction

Human pluripotent stem cell (hPSC) reporter cell lines enable the visualization and isolation of cell types of interest from live cultures for a vast range of downstream applications including RNA-sequencing, proteomics and high throughput screening [1-4]. Used in 3D differentiation systems, such as retinal organoids, they present a powerful method to study both basic developmental processes and disease conditions in a human system. This is vastly superior to alternative approaches such as immortalized cell lines or post-mortem tissue. In the absence of reliable antibodies to a particular target, they often present the only robust tool to visualize specific cell types in fixed cultures. The critical importance of establishing gene reporters in hPSCs is obvious from the absence of alternative model systems for investigating developing human cells and tissues longitudinally. While a treasure trove of different reporter tools exists for the visualization of both rods and cones in murine stem cell-derived organoids, due to the ease with which such tools can be generated, the human pluripotent stem cell system lags behind due to technical difficulties associated with their generation [2-6]. The maturation of genome engineering technologies such as zinc-finger nucleases (ZFN), and in particular the facile CRISPR/Cas9 approach has enabled the generation of pan-photoreceptor and rod reporter tools via the molecular tagging of the *CRX* and *NRL* genes respectively [3, 5-7]. However, no such tools currently exist for human cone photoreceptors, a cell type critical for high acuity and colour vision. To address this paucity and further enable delineation of photoreceptor subtypes in hPSC cultures, we established a cone-specific reporter cell line by tagging the endogenous *GNGT2* locus via a T2A self-cleaving peptide approach. GNGT2 is the cone-specific gamma subunit constituent of Transducin, a heteromeric G-protein protein complex, pivotal to vertebrate phototransduction, linking the G-protein coupled receptor (GPCR) OPSIN to the downstream effector PDE6 and thus regulating the polarisation state of cone photoreceptors [8, 9]. Previously, we confirmed fetal and hPSC expression of *GNGT2* as part of the human cone-enriched gene signature by RNAseq analysis [10] while others have shown early expression in the mouse retina [11]. Fluorescent reporter genes driven by various photoreceptor-specific promoters have demonstrated specific and robust labelling of target cells in rodents and have enabled numerous studies of retinal development, gene profiling, and transplantation [12-17]. To facilitate similar studies focused on cone photoreceptors, equally robust

tools created from hPSCs are required ideally labelling cells throughout development. Here, we describe the generation of a cone-specific *GNGT2* reporter line in the Mastershef7 human embryonic stem cell line [18], using the CRISPR/Cas9 genome-engineering platform. Applying a simplified version of previously described optic vesicle (OV) differentiation protocols, we demonstrate robust production of cones from the GNGT2-T2A-mCherry hESC line that are capable of self-assembling within an organized outer nuclear layer and assuming a mature morphology, as has been shown previously in unmodified hPSC cell lines [17, 19, 20]. We show that GNGT2, a factor typically only associated with the process of phototransduction, is present from the earliest stage of cone development onwards. Furthermore, our novel reporter line reveals that human cones undergo extensive post-mitotic migration within the OV retinal epithelium. Similarly, the human cone population during prenatal development also displays positional changes along the apicobasal axis depending on their state of maturation. The availability of this cone hPSC reporter line, which reliably and innocuously labels human cones throughout their development will be useful for a range of applications of stem cell technology, especially those related to the investigation and treatment of inherited retinal dystrophies.

Material and Methods

ESC culture

The MasterShef7 human embryonic stem cell line, generated by the Centre for Stem Cell Biology, University of Sheffield, was cultured using standard feeder cell free conditions, on Laminin-521 (LN521) (Biolamina) coated flasks (maintenance) or 6 well plates (electroporation, differentiation). Flasks were coated with 5 µg/ml Laminin521 (Biolamina, #LN521) in PBS (+Mg/+Ca2+, PBS Life Technologies, #14190-091) at 4°C O/N or 2h at 37°C. Laminin solution was aspirated and the flask covered with the pluripotent stem cell medium NutriStem XF (Biological Industries, #05-100-1A). Cells were seeded at 10,000 cells/cm^2 and left for 48 h and then fed daily. The cells were passaged every five days at approximately 80% confluency. When passaged the cells were washed twice with PBS (-Mg/-Ca2+, PBS Life Technologies #14190-094), and detached by incubating with a 0.5 mM solution of EDTA (Life Technologies, #15575-020) in PBS-/- for 5 minutes at 37° C. After addition

of 5ml Nutristem XF the cell suspension was centrifuged for 5 minutes at 200g and counted before seeding into a fresh flask.

Generation of the GNGT2_T2A_mCherry targeting vector

The empty pL452 plasmid was obtained from the NCI PRECLINICAL REPOSITORY (USA) and a gBlock (IDT) containing the T2A self-cleaving peptide sequence and mCherry open reading frame, followed by an SV40 polyA signal, was inserted 5' of the loxP-Neo^{R}-loxP cassette. The 5' homology arm, an 882bp gBlock, encompassing GNGT2 exon 4 up to, but not including the TGA termination signal, was cloned into the EcoRV site immediately upstream of T2A-mCherry cassette. The 3' homology arm, a 1000bp gBlock was then cloned into BstX1 site downstream of the loxP-Neo^{R}-loxP cassette. The final donor plasmid was sequenced to confirm the correct sequence and integrity of the repair template. The full plasmid sequence is available in the supplementary section.

CRISPR Cas9 mediated HDR mediated repair

The Benchling CRISPR finder tool was used with default setting to identify sgRNA sequences within 10bp of the GNGT2 TGA termination signal. The GNGT2 sgRNA sequence (GTGGCTGTCTGATAAGCTGA) was cloned under the control of a U6 promoter into a modified version of the chimeric CRISPR plasmid pSpCas9(BB)-2A-Puro (PX459) V2.0 (Addgene, # 62988), in which the ChB promoter was replaced with an EF1α promoter, in order to enhance expression in human pluripotent stem cells. 1x 10^{6} cells were co-electroporated with guide containing Cas9 plasmid (5 µg) and the targeting vector (5 µg) using a BTX ECM 830 electroporator (100V, 5ms, 50ms interval, bipolar pulse). 24h after electroporation the cells were subjected to 400µg G418 (Thermo Fisher, #A1113803) selection for 72h until only single cell clones remained. After a recovery phase of one week, clearly demarcated clones were picked and split individually into two 96 well plates to produce replicates that were then used for either genotyping or clonal expansion. gDNA was extracted using QuickExtract (Lucigen, #QE09050). PCR was performed using spanning primers as well as 5' and 3' primers for genome/construct junctions, which are listed in supplementary table 1. A single 8153 bp band indicates a bi-allelic, 2 bands (8153 bp and 5205 bp) indicate mono-allelic and a single band (5205 bp) indicates no editing (Figure 1C). Out of twelve clones analysed, three showed mono-allelic and one displayed bi-allelic modification of GNGT2. To assess if CRISPR-Cas9 introduced

any off-target mutations we investigated 8 potential genomic locations predicted with Cas OFF finder algorithm (http://www.rgenome.net/cas-offinder/). These were the top hits with highest likelihood of non-specific editing with gRNA1 GTGGCTGTCTGATAAGCTGA. We PCR amplified 200-400 bp region spanning the gRNA binding site and then sequenced to check for possible indels. The sequencing confirmed that no indels were introduced at these genomic locations. Primer sequences and off-target genomic locations are included in supplementary file. Array comparative genome hybridization (array-CGH) was performed using Oxford Gene Technology's (OGT) CytoSure™ Constitutional v3 60K oligo array, according to manufacturer's instructions, using Kreatech's pooled control DNA as a reference (Kreatech Diagnostics, Amsterdam, Holland). Slides were scanned using a G2539A Agilent microarray scanner (Agilent Technologies, Wokingham, UK) and analysed using OGT's CytoSure Interpret (v4.9.40) microarray software.

Retinal differentiation

The GNGT2-T2A-mCherry hESC line was differentiated into retinal organoids using a previously published protocol [21] with minor modifications. Briefly, cells were seeded on LN521 in Nutristem hESC XF media (Biological Industries, #05-100-1A) and allowed to reach near confluence. Once confluent differentiation was initiated by culture in embryoid body media [EB media; DMEM/F12 (Gibco), Knockout serum replacement (Gibco), 1x MEM non-essential amino acids (Gibco), 1x Glutamax (Gibco)] for 72h in the presence of WNT inhibitor 3μM IWR1e (Merck). On day 3, the media was replaced with Neural Induction Medium [NIM; DMEM/F12 (Gibco), 1x MEM non-essential amino acids (Gibco), N2 supplement (Gibco), Heparin (Sigma), 1x Glutamax (Gibco), 3μM IWR1e (Merck)] and feeding continued three times a week to stimulate forebrain development. On day 12 cultures were switched to Retinal Differentiation Medium (RDM; DMEM (Gibco), F12 (Gibco), B27 supplement (Gibco), 1x Glutamax (Gibco) and 10% Fetal Bovine Serum (LifeTech) and cultures fed on alternating days. RDM was supplemented with Taurine (100μM, Sigma), T3 (20nM, Sigma), IGF-1 (5ng/ml, Sigma). After 100 days in culture Retinoic Acid (0.5μM, Sigma) was added to RDM as well. After three weeks, Optic Vesicles (OVs) begin to form which appeared as rounded neuroepithelial structures extending from the monolayer and growing over a patch of cells that form a

retinal pigmented epithelium (RPE). The OVs were manually excised between day 25-35 and cultured in RDM in low attachment 10cm plates.

Human fetal retinae

Human fetal eyes were obtained from the Joint Medical Research Council UK (grant no. G0700089)/Wellcome Trust (grant no. GR082557) Human Developmental Biology Resource (http://www.hdbr.org/). N= 4 eyes, 21 wpc; N=2 eyes, 16 wpc; N=2 eyes, 10wpc.

Immunohistochemistry and quantifications

Samples, comprised of six to ten OVs, were fixed in 4% PFA/PBS for 10 minutes at room temperature and then washed three times in PBS for 10 minutes each. The OVs were then cryopreserved by soaking in a PBS/30% sucrose solution for >1h at room temperature. Embedding was carried out using OCT compound and frozen samples stored at - 80 °C. Frozen blocks were sliced into 18 µm cryosections and transferred on glass slides. OCT compound was removed by a 15 minutes incubation in PBS at 37°C. Sections were then blocked for 1 hour (PBS/0.1% Triton-x, 10% FBS, 1% BSA) followed by an incubation with the primary antibodies overnight at 4°C. The next day, primary antibodies were washed off and the samples were incubated with secondary antibodies for 1 hour at room temperature (supplementary table 6). Slides were then mounted and sealed with nail polish. Images were produced with a Leica SP8 Confocal microscope or Leica DM4B and processed using ImageJ's Cell Counter plugin. OVs from three independent differentiation experiments were collected at different developmental stages and set of ≥3 organoids analysed. For analysis of apical-basal positions of $mCherry^+$ cells within retinal organoids the neuroepithelium was divided into apical and basal halves and scored using ImageJ as above. Quantifications and statistics were performed in GraphPad Prism. Statistical tests are listed in figure legends. All error bars represent the standard error of the mean.

Time-lapse imaging

Retinal organoids (d32-d37) were placed in glass chamber slides (Lab-Tek) and either embedded in 0.1% agarose/PBS or weighted by sterile filter mesh to fix positions of the samples. Organoids were kept in their normal culture medium. Time-lapse imaging was performed either with a Leica SP8 Confocal microscope (LAS X software) or EVOS M5000 system with temperature and $C0_2$ control.

The imaging interval was every 20min or 15min, respectively. Image stacks and movies were generated using ImageJ.

Results

GNGT2-T2A-mCherry hESC line generation. To generate a cone photoreceptor-specific reporter line, we introduced a T2A-mCherry-polyA cassette in frame 3' prime of the endogenous *GNGT2* stop signal in the hESC line Mastershef7 [18], using CRISPR/Cas9-mediated gene editing. The use of a self-cleaving peptide sequence excludes potential confounding phenotypes associated with replacing the endogenous allele or creating a fusion protein [22, 23]. An in-depth description of this approach is provided in the Material and Methods section and is briefly summarized here. A targeting vector was constructed by inserting homology arms containing human *GNGT2* sequence from immediately upstream and downstream of the final codon into a vector containing a T2A-mCherry-polyA cassette, followed by a loxP-flanked neomycin selectable marker (Fig. 1A). The sgRNA was designed in such way as to target sequence within a 10bp window of the homology arms close to the endogenous translation termination signal to increase homology driven repair (HDR) efficiency. Following co-electroporation of the targeting vector with an EF1-Cas9 expressing plasmid, containing the *GNGT2* targeting sgRNA sequence, clones which had incorporated the T2A-mCherry-loxP-neomycin-loxP cassette were identified by resistance to G418. Persisting colonies were analysed by PCR and 4 clones were selected for further analysis. Genotyping was carried out using several primer combinations that distinguished the unedited *GNGT2* loci from successfully targeted ones (Fig. 1B, supplementary table 1). One of the selected clones demonstrated targeted incorporation of the mCherry reporter cassette at both GNGT2 loci (Fig. 1C, Fig. S1). The GNGT2-T2A-mCherry (henceforth referred to as GNGT2mCherry) clone was expanded and partially sequenced to rule out unintended genetic modifications (Fig. S2). To ensure that no off-target mutations were introduced, the top-eight predicted off-sites (crispr.mit.edu) for the sgRNA were amplified and sequenced from the selected clone and no off-target mutations were detected (see supplemental tables 3-5, Fig. S3). Lastly, we performed array comparative genome hybridization (array-CGH) and found that gene editing did not

result in the introduction of any copy number variants (Fig. S4). All subsequent experiments were conducted using this homozygous clone (clone #4).

Generation of OVs from the GNGT2mCherry reporter line. Mastershef7 GNGT2mCherry hESCs were grown to 70 - 90% confluence and subsequently transferred from Nutristem XF media to growth factor-free EB (embryoid body) media (Fig. 1D). On day 3, cells were switched to neural induction medium (NIM) and maintained in the same until day 12 at which point neural rosettes became visible. From day 12 onwards, cultures were maintained in retinal differentiation medium (RDM). Early OV colonies were clearly identifiable by light microscopy by their wheel-like appearance starting from day 20 onwards. Between days 25-35, OVs were excised manually and maintained in suspension for the duration of their time in culture (see Materials and Methods for details of the culture protocol and immunohistochemistry, IHC protocols) (Fig 1E-G). At day 30, OVs consisted mainly of a layer of proliferative PAX6^{+} retina progenitor cells (RPCs) (Fig. 1H) and an inner layer of BRN3a^{+} retinal ganglion cells (Fig. 1I). Organoids displayed a clear apicobasal polarity with ZO-1^{+} (Fig. 1K) cells located on the outside and LAMININ (Fig. 1J) located on the inside. Outer segment-like protrusions from the surface of OVs were visible at d120 and remained readily apparent by light microscopy until the latest stage of analysis (Fig. 1G).

Monitoring cone production in live GNGT2mCherry organoids. mCherry expression was first observed in single cells or small clusters in cultured OVs between day 32-36 of differentiation (Fig. 2A), and increased steadily over time (Fig. 2B-G). Weakly mCherry^{+} cells were mostly located at the apical surface whereas strongly positive cells were situated towards the basal side of the retinal neuroepithelium. By day 70, all organoids displayed strong mCherry expression in a distinctive focal pattern (Fig. 2C-E), which resolved to a uniform coverage of the organoid's surface over time. Robust mCherry fluorescence continued until at least day 152, the latest time point tested (Fig. 2G).

To determine the starting point and location of mCherry expression along the cone developmental axis we analysed organoids from d30 onwards by IHC, using the mitotic markers KI67 and PH3 as well as the cone/horizontal marker ONECUT1. mCherry^{+} cells were first observed at day 32 of differentiation (Fig. 3A). Although, the most strongly positive cells were located near the basal surface of the organoids, weakly positive cells were seen apically as well as at different locations

throughout the retinal epithelium (Fig. 3A-C). At no stage did we observe co-expression with PH3 or KI67 indicating that mCherry expression is restricted to post-mitotic cells (Fig. 3A, B). At day 32 presumptive cone/horizontal precursors, expressing ONECUT1 were located mainly at the apical surface of the neural retina (Fig. 3C). Subsequently, the ONECUT1 expression shifted basally until at d36 most of the cells expressing this marker were residing there. While we found that most, if not all, mCherry$^+$ cells co-expressed ONECUT1 at d36 (Fig. 3D), by d48 (Fig. 3E) this overlap was no longer present suggesting that mCherry$^+$ cells had committed to the cone lineage at this point, as ONECUT1 is only maintained in maturing horizontal cells following cell fate determination [24].

Next, we analysed the expression dynamics and pattern of mCherry over time within the emerging photoreceptor population by comparing it to CRX, the earliest known photoreceptor marker [25], using image analysis tools. At day 32, 14 ± 1.4% of all cells expressed CRX, 26 ± 6.2% of which co-expressed mCherry (Fig. 4A, H). Between d32 and d36 most CRX$^+$ cells were either located at the apical or basal surface but some appeared to be in transit between the two sites. The percentage of CRX$^+$ cells within the forming neural retina increased between day 36 and day 152 from 16.8 ± 3% to 43 ± 3%, a trend mirrored by mCherry expression (Fig. 4H). Similarly, CRX/mCherry co-expression increased from 49 ± 2.7% at day 36, to 82 ± 12% at day 70. Consistent with previous findings, these observations indicate that early-mid stage CRX$^+$ cells represent mainly cone photoreceptors rather than rods, which only form during later stages of development [26, 27].

Interestingly, during the day 36 to day 70 time-interval, we observed a notable positional shift of CRX and mCherry$^+$ cells towards the apical surface (Fig. 4B-D), reversing the trend seen at the earlier stages of differentiation (Fig. 4I). By day 152, most of the photoreceptors were located apically suggesting apical migration occurs during cell maturation (Fig. 4G). Consistent with our immunohistochemical analysis, time-lapse imaging carried out at d32 showed mCherry$^+$ descending towards the basal surface (Fig. 4J, Movie 1) while at d37 we observed cell migration towards the apical side (Movie 2).

Fidelity of mCherry expression during OV differentiation. To evaluate the specificity of expression of the GNGT2mCherry reporter line, we compared localization of mCherry to that of endogenous GNGT2, using IHC (Fig. 5). While only 36 ± 13% of mCherry expressing cells co-

labelled with the GNGT2 antibody at day 36 (Fig. 5A, E) this overlap increased to 73 ± 13% by day 70 (Fig. 5B, E) and eventually reached 84 ± 9% by d152 (Fig. 5D, E). Similar to the endogenous protein, mCherry, reflecting transcriptional activity at this locus, showed extensive cytoplasmic labelling of cones including cell projections and extensions, and also included, by day 152, thick cone segments (Fig. 5D). These results confirm that the GNGT2mCherry line robustly recapitulates endogenous *GNGT2* expression throughout retinal differentiation in OV cultures.

Expression of late photoreceptor markers in mCherry$^+$ cells. To further examine the characteristics of mCherry expression in maturing photoreceptors the distribution of late markers was analysed via IHC. The pan-photoreceptor neuronal calcium-binding protein RECOVERIN was observed in 76% of mCherry$^+$ cells at day 70 (data not shown) and labelled most of those cells by day 120 (Fig. 6A), suggesting a slightly delayed onset of expression relative to GNGT2. Consistent with previous reports, blue-sensitive OPSIN (OPN1SW) was weakly expressed in a small number of mCherry$^+$ cells at day 120 (data not shown), but showed a robust staining of those cells, in particular their segments, by day 152 (Fig. 6B). Despite the strong expression of this late marker in some cells, the overall number of OPN1SW$^+$ cones within the mCherry$^+$ population remained very low (0.45%). In contrast, the red cone photopigment OPN1LW, a marker of mature long wave sensitive cones, was present in 26.25±13% of all mCherry expressing cells at day 152 of differentiation showing a distinct staining pattern in cone cell bodies, segments and processes (Fig. 6C). Interestingly, the biased production of OPN1LW$^+$ at the expense of OPN1SW$^+$ cones is in line with observations from a previous study in which T3 was added to the culture media early on in differentiations [28].

Further confirming the status of the GNGT2mCherry reporter as an early cone marker, most if not all mCherry$^+$ cells at this stage also expressed Cone Arrestin (ARR3) and Retinoic Acid Receptor Gamma (RXRγ) (Fig. S5A, B).

Lastly, we assessed the localization of the rod markers NR2E3 and RHODOPSIN in organoid sections by IHC. Rods, labelled by NR2E3, were well established at day 152, typically located basal to cone cell bodies (Fig. 6D). RHODOPSIN labelling was absent in organoids prior to day 120 (data not shown), but showed a consistent apical staining in some photoreceptor segments by day 152 (Fig. 6E). In contrast to relatively thick segments observed in GNGT2mCherry$^+$ cells, RHODOPSIN was

restricted to comparatively thin segments as seen typically in vertebrate rod photoreceptors. Furthermore, RHODOPSIN staining seen in cell bodies was very weak compared to the levels observed in segments and was completely absent from mCherry^{+} cells. Our data thus confirms that mCherry, as expected, efficiently labels cone subtypes, but not rod photoreceptors.

Dynamics and pattern of cone marker expression in the human fetal retina.

During retinal histogenesis cone photoreceptors are born at the apical surface of the developing retina and later reside at the most apical side of it [29]. As the birth-site and final residence of these cells are both at the most apical location, it has long been assumed that human cone photoreceptors do not need to translocate substantially after they exit cell cycle. However, our GNGT2mCherry reporter line suggests cones undergo extensive migratory movements along the radial axis of retinal organoids. Our analysis of different stages of organoid differentiation and time-lapse imaging is consistent with a pattern of cone cell movement in which weakly mCherry^{+} immature cones cells form at the apical surface and then descend basally during which time reporter expression increases significantly, suggesting progressive maturation along the cone lineage. During the time window between day 48 and day 70 in organoids, the location of the majority of cones then shifts back apically to assume their final position in the forming outer nuclear layer (ONL). In order to examine if this putative migratory behaviour seen in our stem cell-derived retinal organoids reflects that seen *in vivo*, or represents an *in vitro* artefact, we analysed the distribution of developing cones in the human fetal retina, using a panel of known cone markers. Mammalian retinas mature in a central to peripheral fashion, meaning that centrally located cones are further along their developmental program compared to their peripheral counterparts [30]. IHC analysis of 21 week post conception (wpc) human retinae using the early cone marker RXRγ showed that robustly labelled RXRγ^{+} cones always occupied the most apical location in the ONL independent of their position on the central-peripheral axis (Fig. 7A, B, C). Weak RXRγ expression also labelled cells throughout the retina. Next, we assessed the location of GNGT2^{+} cones and found strong cytoplasmic labelling in cones at the most apical locations in both peripheral and mid-peripheral locations in the fetal retina (Fig. 7D, E, Fig. S6A). In the central retina, however, we observed labelling of cones at various locations along the radial axis, usually displaying prominent end feet at the presumptive outer plexiform layer as well as at the apical surface (Fig. 7F, Fig. S6D).

This pattern of expression was mirrored by cones expressing either long-wave (OPN1LW) or short-wave (OPN1SW) sensitive cone OPSINS (Fig. 7G-L, Fig. S6B, C and E, F, respectively). Of note, more OPN1SW expressing cells appeared peripherally compared with their LW-sensitive counter parts, in agreement with the fact that they arise earlier in histogenesis [28, 31]. Interestingly, in the mid-periphery, apically located OPN1^{+} cones were frequently observed extending processes towards the outer plexiform layer (Fig. 7H, K and Fig. S6B, C) suggesting an active migratory process rather than a simple displacement of cone somata. Furthermore, cones in 16wpc retinae were always restricted to the apical surface and did not display any basal processes, suggesting that any somal translocation would occur between this time point and 21wpc when many cone somata are found at basal positions within the ONL (Fig. S7).

Taken together, our analyses show that human fetal cones assume different positions along the apicobasal axis in the retina depending on their developmental age, consistent with the migratory movements observed with GNGT2mCherry-expressing cones in our hESC derived retinal organoids.

Discussion

In this study, we have created the first cone-specific hPSC reporter line using CRISPR/Cas9 tools by introducing a T2A-mCherry cassette into the endogenous human *GNGT2* locus, a strategy that ensures faithful capitulation of *GNGT2* expression without any detrimental effects. This targeted knock-in strategy avoids the creation of a non-functional *GNGT2* allele by use of a T2A self-cleaving peptide sequence between the GNGT2 and mCherry reading frames. Consistent with other recent studies [6, 27] we chose not to remove the loxP flanked PGK-Neo selection cassette, however, it should be noted that this could, under certain circumstances, influence the expression levels of nearby genes [32].

The Mastershef7 GNGT2mCherry ESC line strongly labels GNGT2^{+} cones throughout OV differentiation, demarcating the entire cell from axon terminal to segment. The first mCherry^{+} cones arose at day 32 in differentiating OVs, consistent with the time course of human cone development

[33-35]. We found no overlap between mCherry expression and markers of mitotically active cells (PH3, KI67) or progenitor markers (PAX6) demonstrating that labelled cells represent post-mitotic, committed cones. The fact that we nevertheless observed temporary co-expression of mCherry with ONECUT1, a transient marker of bi-potential cone/horizontal progenitors and later only horizontal cells, suggests that *GNGT2*, and hence the reporter, is turned on very shortly after commitment to the cone lineage. mCherry expression preceded GNGT2 protein appearance, but, over time, demonstrated complete overlap. Furthermore, our immunohistochemical analysis using a panel of rod and cone specific antibodies confirms that mCherry expression is restricted to cone photoreceptors and is completely absent from rods. This observation was expected as GNGT2 has been shown to be a constituent of the cone Transducin complex involved in the phototransduction cascade in these cells [8, 36].

While a recent study in rodents, using *in situ* hybridization, showed that *Gngt2* was expressed relatively early in retinal histogenesis, the onset of mCherry expression soon after exit from mitosis, reflected by transient co-expression with ONECUT1, was nevertheless surprising and highlights the sensitivity of our approach [11]. Our new reporter line thus specifically labels cones along their entire post-mitotic developmental axis.

Constituting the γ-subunit of the heterotrimeric G-protein complex Transducin, GNGT2 is thought to play a critical role in vertebrate phototransduction, linking the photopigment Opsin to the downstream effector phosphodiesterase and thus controlling the polarization state of cones via cGMP gated ion channels [36]. Interestingly, while GNGT2 reporter expression, as well as protein, are present by d36 in OVs, the phototransduction pathway itself does not appear to fully assemble until at least 3 months later based on late marker expression such as OPN1LW [28]. It is thus tempting to speculate that GNGT2 carries out additional functions during early cone differentiation as part of a G-protein complex. However, further studies will be required to elucidate any potential role of this factor during this dynamic time of cone development characterized by transcriptional, morphogenetic as well as positional changes.

Furthermore, analysis of fluorescently labelled cones in OVs indicated extensive migratory activity occurs along the radial OV axis with the weakly mCherry^{+} cells appearing apically before descending

towards the basal lamina and eventually returning to the apical surface, where they contributed to the forming ONL. Using human fetal retinae, we observed that mCherry^{+} cones in OVs recapitulate similar migratory movement patterns seen *in vivo* albeit with differences in timing. Fetal cones in the retinal periphery and mid-periphery, a less mature environment compared to the central retina, were restricted to the most apical aspect of the developing ONL. In contrast, we observed that along the peripheral-central axis cones took up progressively more basal positions within the ONL, thus mirroring the movement patterns observed in organoids. It is known that retinal progenitors undergo extensive interkinetic nuclear migration, in which nuclei show characteristic apico-basal movements with mitosis occurring at the apical side and DNA synthesis taking place basally [29, 37]. While post-mitotic movements of cone nuclei have been reported in mice, the signals and molecular pathways controlling this process have not been resolved [38, 39]. A study of ectopically located cones in GRF2-KO mice suggested a potential role for GRF2 and CDC42 in the formation/structure of PAR-containing, polarity-related macromolecular complexes [40, 41], and the serine/threonine kinase LKB1 as well as one of its substrates, AMPK, have also been identified as regulators of cone nuclear positioning [42]. Our observations suggest that in human retinae apical cones extend processes basally, prior to relocation, in an active process rather than one based on simple somal displacement by newly generated rods. Understanding the exact molecular mechanisms governing cone photoreceptor migration will not only contribute to a better understand of how the retinal architecture assembles, but will also be critical to the development of cell therapy strategies for the treatment of inherited retinal dystrophies.

Conclusions

Taken together, our novel GNGT2mCherry reporter hESC reporter line labels human cones in OVs robustly and reliably, recapitulating endogenous *GNGT2* expression along the entire timeline of cone development. It thus represents a valuable tool for a broad range of basic and translational studies, using hPSC-OV technology. For example, the ability to specifically label all cones provides a platform to study human photoreceptor development or test protocols that bias towards particular photoreceptor fates. Using this novel tool, it will be possible to introduce mutations in retinal

dystrophy genes, allowing reliable assessment of cone-specific outcomes (retinitis pigmentosa, cone degeneration etc.) relative to the unedited, isogenic reporter line. Access to an unrestricted supply of fluorescently labelled, hPSC-derived cones may also accelerate the development of cell replacement strategies for patients with retinal degenerative diseases, as these cells could be used in proof-of-concept studies and for tracking cone fate post-transplantation in rodent models.

DATA AVAILABILITY STATEMENT

The data that support the findings of our study are available from the corresponding author upon reasonable request.

DISCLOSURE

All of the authors declared no potential conflicts of interest.

Figure Captions

Figure 1. Production of the GNGT2mCherry hESC line. (**A**) Targeting vector map. An ATG-less mCherry coding sequence was fused via a T2A site to the GNGT2 open reading frame (not including stop signal), followed by the SV40 polyA terminator and a loxP-flanked neomycin (NeoR) selection cassette. GNGT2 homology arms flanked the reporter on either side. (**B**) Schematic of an unedited GNGT2 allele (top), and a GNGT2 allele with the mCherry reporter and NeoR selection cassette inserted (bottom). Spanning primers (FW1-RV1) as well as those amplifying 5' (FW1-RV2) and 3' (FW2-RV1) junctions are shown along with expected amplicon lengths. (**C**) Image of agarose gel of genomic PCR products obtained using spanning or junction primers (see 1B). Lane 1-2: Upper 8.1kb band indicates successful targeting while lower 5.2kb band represents unmodified allele. Lane 1 shows that clone #4 is homozygous for the gene targeting at the GNGT2 locus compared to parental wild-type (WT) control hESC line. Lane 3 and 4 show 5' and 3' junctions from clone 4, respectively.

(**D**) Overview of retinal differentiation protocol. (**E-G**) The GNGT2mCherry hESC line generates OVs displaying the typical wheel morphology. (**H, I**) At d30, OVs consist mainly of $PAX6^+$ retinal progenitors (**H**) and internal BRN3a (**I**) expressing ganglion cells. (**J-L**) GNGT2mCherry OVs display typical apical (ZO-1, mitotic (M) phase marker phosphohistone H3, PH3; outside) basal (Laminin; inside) polarity. OVs, optic vesicle. Scale bars = 100 µm (E, F, G, J, K, L), 20 µm (H, I).

Figure 2. Observing cone photoreceptor production in live GNGT2mCherry retinal organoids. Epifluorescence images of live GNGT2mCherry OVs captured over time in differentiation cultures. (**A, B**) Single cells and small patches of $mCherry^+$ cells were detected starting around 4 weeks of culture (d36; arrows in **A**). (**C-F**) By d70 reporter fluorescence was robustly present throughout all OVs, forming discrete patches of $mCherry^+$ cells on the apical surface (white box, **D**). (**E**) High magnification image of box shown in **D**. (**F**) Side view of d70 organoid. (**G**) By d152, GNGT2mCherry appeared uniformly distributed across the OVs. OVs, optic vesicle. Scale bar = 100 µm.

Figure 3. Characterization of early onset and location of GNGT2mCherry expression. Cryosectioned OVs from d32-d48 analysed for location of GNGT2mCherry reporter expression and by immunohistochemistry for progenitor markers KI67, PH3 and bi-potential cone-horizontal precursor marker ONECUT1. (**A-E**) At d32 mCherry $^{+}$ cells were located in both apical and basal regions of the forming neural retina. Proliferative, KI67^{+} cells do not express mCherry (asterisk in A), and occupy apical to central positions along the radial axis. (**B**) Phosphohistone H3 expressing cells undergoing mitosis are restricted to the apical surface and do not express mCherry (arrow). (**C-E**) At d32, ONECUT1 staining is mainly observed in mCherry^{+} cells located at the apical surface consistent with its proposed role in cone fate choice, which takes place there shortly before exit from cell cycle. (**D**) By d36, ONECUT1 expression has shifted basally with few positive cells remaining at the apical surface (arrows). mCherry signal intensity is low in apically located cells (arrows), whereas fluorescence is upregulated in cells near the basal surface, partially overlapping with ONECUT1 staining (arrowheads). (**E**) ONECUT1 and mCherry signals are mutually exclusive by d48 (arrowheads). Scale bar = 20 μm.

Figure 4. Photoreceptor specificity and expression pattern of GNGT2mCherry during retinal differentiation. (**A-G**) Co-immunohistochemistry of pan-photoreceptor (PR) marker cone-rod homeobox, CRX and GNGT2mCherry. (**A**) Co-labelling of mCherry and CRX is observed shortly after the appearance of the first weakly mCherry^{+} cells around d32. Arrow points to an apically located PR while arrowhead indicates PR cell at the basal surface. (**B**) Reporter fluorescence increases towards d36 and double positive cells are visible at various locations along the apical-basal axis (arrow, apical; asterisk, central; arrowhead, basal). (**C, D**) Between d48 and d70, a basal to apical shift of the CRX/mCherry^{+} population is observed. (**D-G**) After d70, most of the CRX/mCherry photoreceptors reside near the apical surface where they assemble a nascent outer nuclear layer, which compacts by d152. (**H**) Quantification of CRX and GNGT2mCherry expression in OVs during differentiation. While CRX expression always preceded that of mCherry the latter is highly specific not showing any expression in non-photoreceptor cells. (**I**) Apicobasal positions of mCherry^{+} cells within the organoid neuroepithelium. Locations of mCherry^{+} cells shift from basal to apical halves

over time. Pearson correlation coefficient R=0.94, P-Value is 0.018. (**J**) Time-lapse images corresponding to supplementary movie 1 show migration of mCherry$^+$ cells towards basal side. Scale bar = 25 μm. Error bars are SEM.

Figure 5. Assessment of GNGT2mCherry fidelity.

(**A-D**) Immunohistochemical analysis of mCherry expression using an anti-GNGT2 antibody. Co-labelling (arrows) is present by d36 in mCherry$^+$ photoreceptors (36 ± 13.4%). Arrowhead indicates mCherry$^+$ cells, which do not yet express GNGT2 protein. (**B-E**) The number of mCherry$^+$ cells also displaying GNGT2 immunoreactivity increases over time in OVs (73 ± 13.2%, d70; 83.5 ± 9%, d152). (**D**) By day 152 cells adopt typical cone morphology with both fluorescent reporter and immunolabelling visible throughout the cell body, particularly marking the thick photoreceptor segments (arrows). (**E**) Quantification of mCherry/GNGT2 co-labelling during OV differentiation. GNGT2 immuno labelling is always observed as a subset of mCherry expression. Error bars are SEM. Scale bar = 25 μm.

Figure 6. Evaluation of cone lineage specificity. Immunohistochemical analysis of OVs using photoreceptor maturation markers. (**A)** Expression of calcium binding protein RECOVERIN labels most if not all mCherry positive photoreceptors by d120. (**B, C**) Expression of the late cone markers OPN1SW (**B**) and OPN1LW (**C**) was restricted to mCherry$^+$ photoreceptors at the most apical aspect of the outer nuclear layer at d152 of differentiation (arrows). OPN1LW is visible throughout the cell body, while OPN1SW is mainly localized to apical segment-like structures. (**D**) NR2E3 positive rods do not co-express GNGT2/mCherry (arrows). Inset shows high magnification view of dashed box. (**E**) Rod photoreceptor pigment RHODOPSIN is present in some photoreceptor segments (arrow), but does not co-localize with mCherry. Inset shows high magnification view of boxed area. Scale bar = 25 μm (A, B, E), 10 μm (C, D).

Figure 7. Evaluation of cone cell positions in the fetal human retina. (**A-L**) Immunohistochemical analysis of cone markers (RXRγ, GNGT2, OPN1LW, OPN1SW) in the peripheral, mid-peripheral and central 21wpc human retina. (**A-C**) Throughout the retina, RXRγ labelling is most prominent in

presumptive immature cones located at apical positions within the ONL. Cones in the developmentally immature periphery (**A, D, G, J**) and mid-periphery (**B, E, H, K**) assume positions at the apical surface, directly abutting the RPE (arrows). (**H, K**) Apically located OPN1LW^{+} and OPN1SW^{+} cones in the mid-periphery extend end feet bearing processes (asterisks) towards the nascent outer plexiform layer. (**F-L**) Insets show high magnification view of cones labelled with yellow arrows. Arrowheads point to end foot of basal process (BP). **(F, I, L)** In the central retina, the most mature part of the tissue, cone cell bodies are visible at various positions along the apical-basal axis of the outer nuclear layer (arrows), often displaying thick end foot labelling near the OPL and OLM. Outer nuclear layer, ONL; outer plexiform layer, OPL (dashed line); outer limiting membrane, OLM. Scale bar = 20 μm (A-I), 10 μm (L) and 50 μm.

1. Shimada, H., et al., *In Vitro Modeling Using Ciliopathy-Patient-Derived Cells Reveals Distinct Cilia Dysfunctions Caused by CEP290 Mutations.* Cell Rep, 2017. **20**(2): p. 384-396.
2. Sluch, V.M., et al., *Differentiation of human ESCs to retinal ganglion cells using a CRISPR engineered reporter cell line.* Sci Rep, 2015. **5**: p. 16595.
3. Kaewkhaw, R., et al., *Transcriptome Dynamics of Developing Photoreceptors in Three-Dimensional Retina Cultures Recapitulates Temporal Sequence of Human Cone and Rod Differentiation Revealing Cell Surface Markers and Gene Networks.* Stem Cells, 2015. **33**(12): p. 3504-18.
4. Krentz, N.A.J., et al., *Single-Cell Transcriptome Profiling of Mouse and hESC-Derived Pancreatic Progenitors.* Stem Cell Reports, 2018. **11**(6): p. 1551-1564.
5. Phillips, M.J., et al., *Generation of a rod-specific NRL reporter line in human pluripotent stem cells.* Scientific Reports, 2018. **8**.
6. Collin, J., et al., *Using Zinc Finger Nuclease Technology to Generate CRX-Reporter Human Embryonic Stem Cells as a Tool to Identify and Study the Emergence of Photoreceptors Precursors During Pluripotent Stem Cell Differentiation.* Stem Cells, 2016. **34**(2): p. 311-21.
7. Gagliardi, G., et al., *Characterization and Transplantation of CD73-Positive Photoreceptors Isolated from Human iPSC-Derived Retinal Organoids.* Stem Cell Reports, 2018. **11**(3): p. 665-680.
8. Ong, O.C., et al., *Gene structure and chromosome localization of the G gamma c subunit of human cone G-protein (GNGT2).* Genomics, 1997. **44**(1): p. 101-9.
9. Larhammar, D., K. Nordstrom, and T.A. Larsson, *Evolution of vertebrate rod and cone phototransduction genes.* Philos Trans R Soc Lond B Biol Sci, 2009. **364**(1531): p. 2867-80.
10. Welby, E., et al., *Isolation and Comparative Transcriptome Analysis of Human Fetal and iPSC-Derived Cone Photoreceptor Cells.* Stem Cell Reports, 2017. **9**(6): p. 1898-1915.
11. Rodgers, H.M., et al., *Embryonic markers of cone differentiation.* Mol Vis, 2016. **22**: p. 1455-1467.
12. Borsch, O., T. Santos-Ferreira, and M. Ader, *Photoreceptor Transplantation into the Degenerative Retina.* Klinische Monatsblatter Fur Augenheilkunde, 2017. **234**(3): p. 343-353.
13. Decembrini, S., et al., *Cone Genesis Tracing by the Chrnb4-EGFP Mouse Line: Evidences of Cellular Material Fusion after Cone Precursor Transplantation.* Mol Ther, 2017. **25**(3): p. 634-653.
14. Eberle, D., et al., *Subretinal Transplantation of MACS Purified Photoreceptor Precursor Cells into the Adult Mouse Retina.* Jove-Journal of Visualized Experiments, 2014(84).
15. Eberle, D., et al., *Increased Integration of Transplanted CD73-Positive Photoreceptor Precursors into Adult Mouse Retina.* Investigative Ophthalmology & Visual Science, 2011. **52**(9): p. 6462-6471.
16. Lakowski, J., et al., *Cone and rod photoreceptor transplantation in models of the childhood retinopathy Leber congenital amaurosis using flow-sorted Crx-positive donor cells.* Human Molecular Genetics, 2010. **19**(23): p. 4545-4559.
17. Gonzalez-Cordero, A., et al., *Recapitulation of Human Retinal Development from Human Pluripotent Stem Cells Generates Transplantable Populations of Cone Photoreceptors.* Stem Cell Reports, 2017. **9**(3): p. 820-837.
18. Canham, M.A., et al., *The Molecular Karyotype of 25 Clinical-Grade Human Embryonic Stem Cell Lines.* Sci Rep, 2015. **5**: p. 17258.
19. Meyer, J.S., et al., *Modeling early retinal development with human embryonic and induced pluripotent stem cells.* Proc Natl Acad Sci U S A, 2009. **106**(39): p. 16698-703.
20. Reichman, S., et al., *From confluent human iPS cells to self-forming neural retina and retinal pigmented epithelium.* Proc Natl Acad Sci U S A, 2014. **111**(23): p. 8518-23.
21. Cuevas, E., et al., *NRL(-/-) gene edited human embryonic stem cells generate rod-deficient retinal organoids enriched in S-cone-like photoreceptors.* Stem Cells, 2021. **39**(4): p. 414-428.

22. Trichas, G., J. Begbie, and S. Srinivas, *Use of the viral 2A peptide for bicistronic expression in transgenic mice.* BMC Biol, 2008. **6**: p. 40.
23. Kim, J.H., et al., *High cleavage efficiency of a 2A peptide derived from porcine teschovirus-1 in human cell lines, zebrafish and mice.* PLoS One, 2011. **6**(4): p. e18556.
24. Emerson, M.M., et al., *Otx2 and Onecut1 promote the fates of cone photoreceptors and horizontal cells and repress rod photoreceptors.* Dev Cell, 2013. **26**(1): p. 59-72.
25. Hennig, A.K., G.H. Peng, and S. Chen, *Regulation of photoreceptor gene expression by Crx-associated transcription factor network.* Brain Res, 2008. **1192**: p. 114-33.
26. Cepko, C.L., et al., *Cell fate determination in the vertebrate retina.* Proc Natl Acad Sci U S A, 1996. **93**(2): p. 589-95.
27. Collin, J., et al., *CRX Expression in Pluripotent Stem Cell-Derived Photoreceptors Marks a Transplantable Subpopulation of Early Cones.* Stem Cells, 2019. **37**(5): p. 609-622.
28. Eldred, K.C., et al., *Thyroid hormone signaling specifies cone subtypes in human retinal organoids.* Science, 2018. **362**(6411).
29. Amini, R., M. Rocha-Martins, and C. Norden, *Neuronal Migration and Lamination in the Vertebrate Retina.* Frontiers in Neuroscience, 2018. **11**.
30. Prada, C., et al., *Spatial and Temporal Patterns of Neurogenesis in the Chick Retina.* Eur J Neurosci, 1991. **3**(11): p. 1187.
31. Hoshino, A., et al., *Molecular Anatomy of the Developing Human Retina.* Dev Cell, 2017. **43**(6): p. 763-779 e4.
32. Pham, C.T., et al., *Long-range disruption of gene expression by a selectable marker cassette.* Proc Natl Acad Sci U S A, 1996. **93**(23): p. 13090-5.
33. Hendrickson, A., et al., *Rod photoreceptor differentiation in fetal and infant human retina.* Exp Eye Res, 2008. **87**(5): p. 415-26.
34. Xiao, M. and A. Hendrickson, *Spatial and temporal expression of short, long/medium, or both opsins in human fetal cones.* J Comp Neurol, 2000. **425**(4): p. 545-59.
35. Hendrickson, A. and C. Zhang, *Development of cone photoreceptors and their synapses in the human and monkey fovea.* J Comp Neurol, 2019. **527**(1): p. 38-51.
36. Arshavsky, V.Y., T.D. Lamb, and E.N. Pugh, Jr., *G proteins and phototransduction.* Annu Rev Physiol, 2002. **64**: p. 153-87.
37. Quinn, P.M.J. and J. Wijnholds, *Retinogenesis of the Human Fetal Retina: An Apical Polarity Perspective.* Genes (Basel), 2019. **10**(12).
38. Rich, K.A., Y. Zhan, and J.C. Blanks, *Migration and synaptogenesis of cone photoreceptors in the developing mouse retina.* J Comp Neurol, 1997. **388**(1): p. 47-63.
39. Smiley, S., et al., *Establishment of a cone photoreceptor transplantation platform based on a novel cone-GFP reporter mouse line.* Sci Rep, 2016. **6**: p. 22867.
40. Jimeno, D., et al., *RASGRF2 controls nuclear migration in postnatal retinal cone photoreceptors.* J Cell Sci, 2016. **129**(4): p. 729-42.
41. Jimeno, D. and E. Santos, *A new functional role uncovered for RASGRF2 in control of nuclear migration in cone photoreceptors during postnatal retinal development.* Small GTPases, 2017. **8**(1): p. 26-30.
42. Burger, C.A., et al., *LKB1 and AMPK instruct cone nuclear position to modify visual function.* Cell Rep, 2021. **34**(5): p. 108698.

Lakowski, Figure 1, top

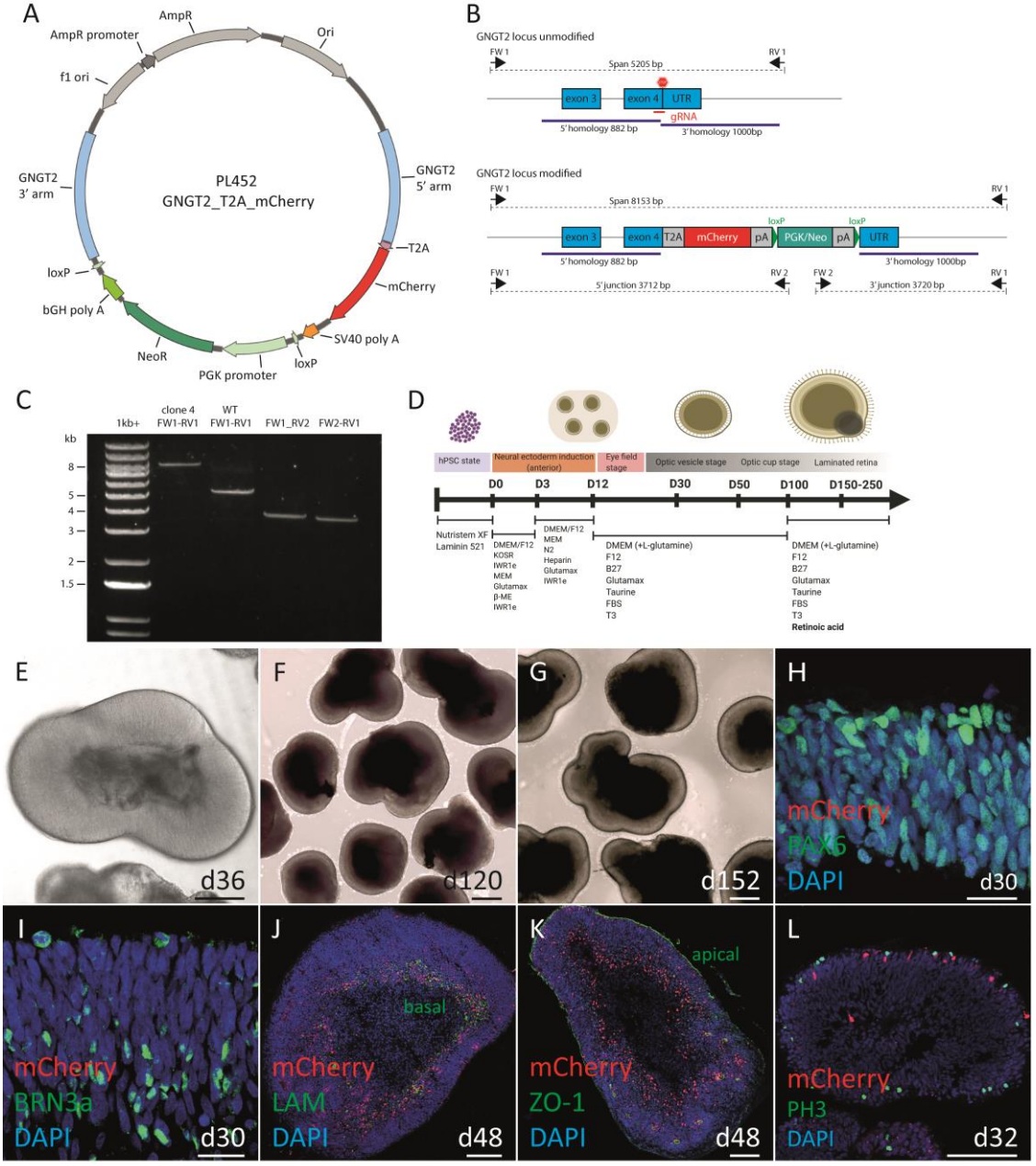

Lakowski, Figure 2, top

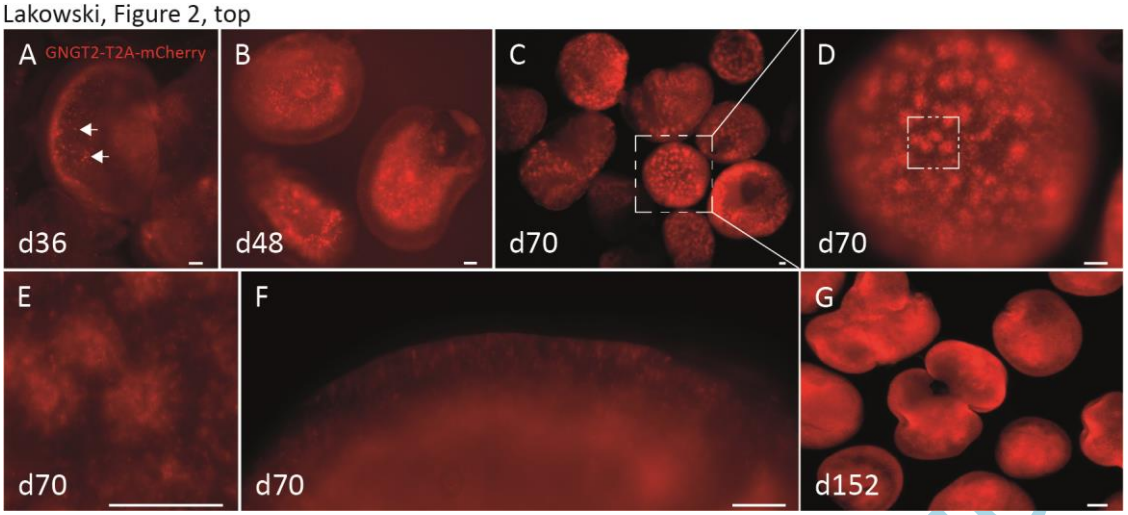

Lakowski, Figure 3, top

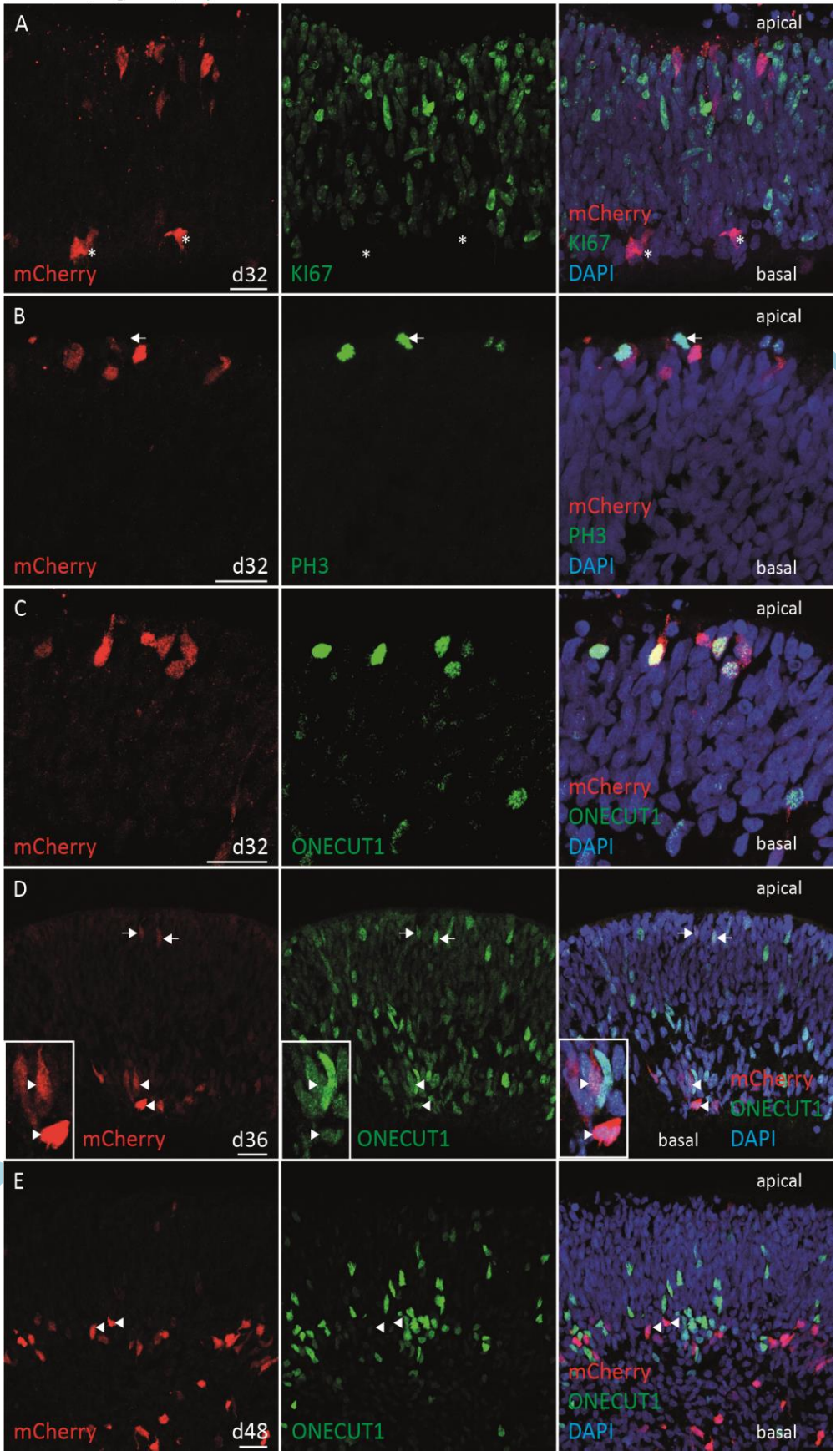

Lakowski, Figure 4, top

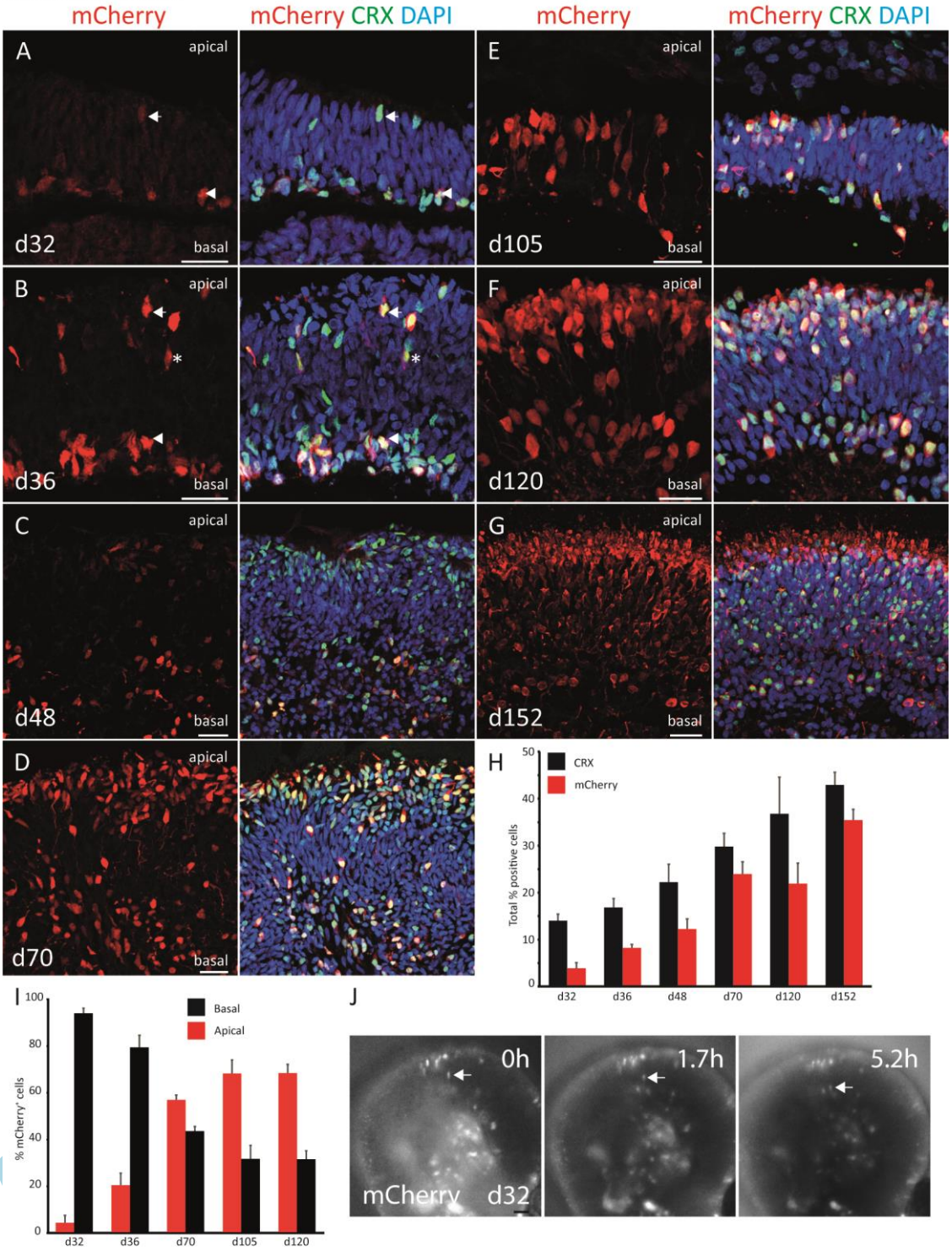

Lakowski, Figure 5, top

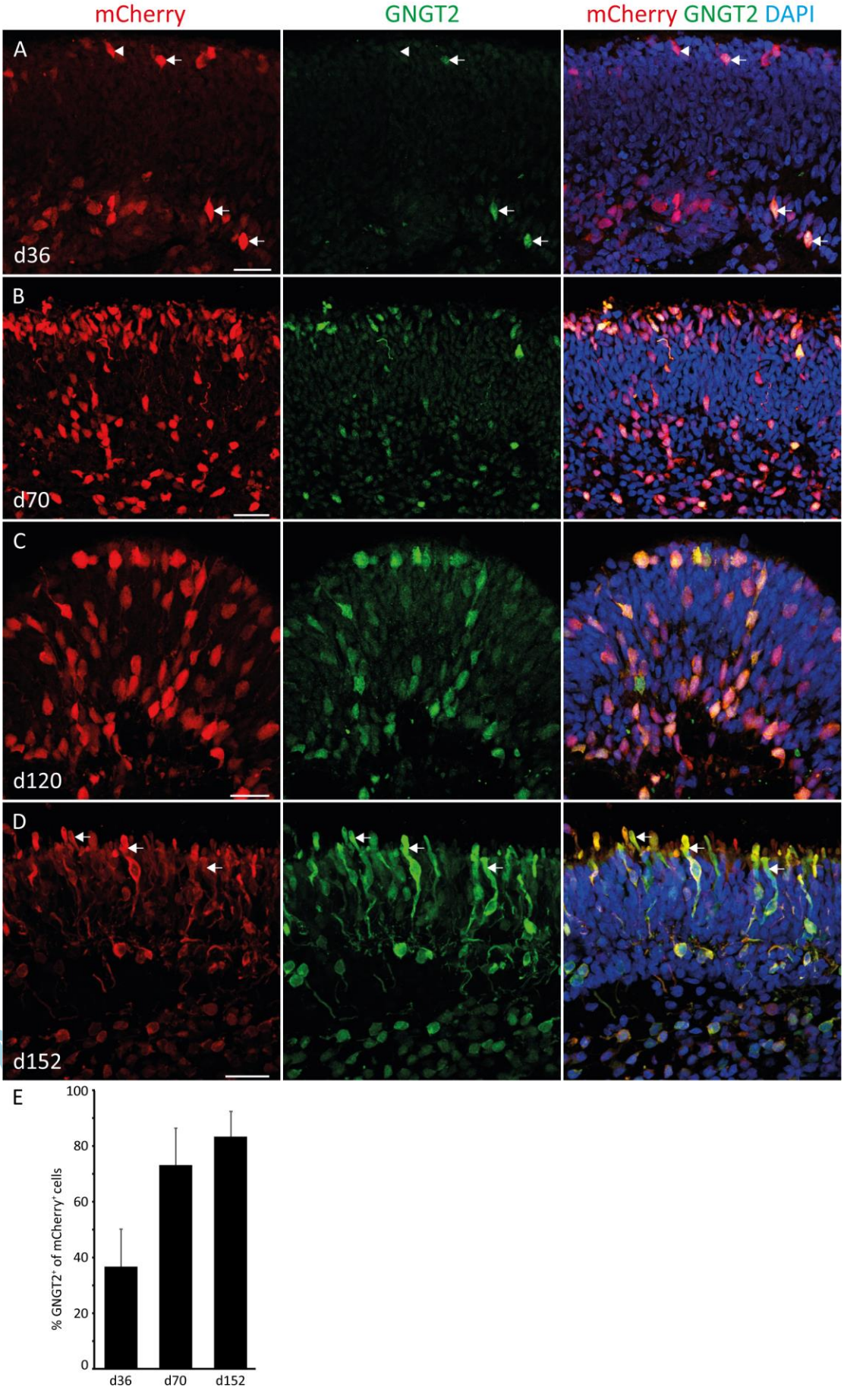

Lakowski, Figure 6, top